THEORETICAL AND APPLIED MECHANICS
Volume 49 (2022) Issue 1, 1–14 DOI: https://doi.org/10.2298/TAM211103002T

AUXETIC METAMATERIALS SUBJECTED TO DYNAMIC LOADINGS

Georgios K. Tairidis†, Ioannis Ntintakis, Georgios A. Drosopoulos, Panagiotis Koutsianitis, and Georgios E. Stavroulakis

Abstract. Materials with negative Poisson's ratio are called auxetics and they present enhanced properties (e.g. damping, indentation resistance, fracture toughness and impact resistance) under external loadings. The auxetic properties are derived from peculiar-shaped microstructures, such as star-shaped frames. In the present investigation, several applications are studied using auxetic microstructures. Finite element models are developed for dynamic analysis. First, an application related to auxetic microstructures, for the core of structural panels, is presented. Next, the use of auxetic materials in armor plates in dynamic bullet penetration problems is considered. Finally, a numerical simulation for wind turbines blades, with aluminum foam, polymeric foam and the proposed auxetic material is carried out. The numerical results demonstrate that the use of auxetic microstructures results in improved dynamic response of the system in comparison to conventional materials.

1. Introduction

Mechanical metamaterials with a negative Poisson's ratio are called auxetic materials or simply auxetics. Auxetic materials have enhanced dynamical properties and damping behavior, and thus they can be used in the field of biomechanics, in manufacturing of woven components with special mechanical properties, in energy absorption applications and others. This property is usually explained from the microstructure (e.g. star-shaped frames or inclusions), although other models have been used as well, such as chiral or mechanism-based models [16].

Auxetic materials are used in several fields; however, optimal design towards dynamical properties is still under investigation. A modern approach to design auxetics is based on topology optimization methods. Nevertheless, even classical auxetic microstructures may be used, possibly after tuning, for certain applications.

2020 *Mathematics Subject Classification:* Primary 74M25; Secondary 74H45; 74S05.
Key words and phrases: auxetic materials, frequency analysis, dynamic analysis, negative Poisson's ratio.

† Died, February 20, 2022. His early and unexpected death brings great sadness to his family and his colleagues.

A first effort to review the effect of auxetic metamaterials in applications with dynamic loadings is attempted in the present paper.

A particularly important application field is the use of auxetic materials in protection equipment, for infrastructures, vehicles and bodies. The additive manufacturing has a significant contribution to the construction of body armor. The construction of the auxetic structures using conventional production methods is often unfeasible as they are characterized by geometry of high complexity. Yang et al. in [17] studied the potential uses of re-entrant hexagon and arrowhead type printed auxetic structures made from common polymers in order to be used in body protection. Moreover, Imbalzano et al. in [6–8] investigated the blast resistance of hybrid sandwich panels. In addition, Han et al. in [5] created two structures of auxetic materials for high absorption of energy, and Alomarah et al. in [1] studied the in-plane mechanical properties of auxetic structures subjected to dynamic compression experimentally and numerically. The effectiveness of sandwich structure with auxetic 3D re-entrant lattice core and semi-auxetic braided composite face sheets subjected to high-velocity impact has been investigated in [12]. The auxetic behavior of materials in engineering applications is discussed in [13]. The present paper is outlined as follows: in the first part of the study, a short literature review on classical auxetic microstructures, which still have potential for further applications, as well as hints for more complicated optimal design methods, are provided. Consequently, three different numerical experiments are carried out. The first one studies a damping plate with conventional and auxetic materials on damping panels. Next, a comparative evaluation of a star-shaped auxetic and a non-auxetic structure under high-velocity impact is discussed (cf [14]). Finally, an application of auxetic metamaterials on a wind turbine blade is presented. The results obtained from the numerical experiments allow us to draw preliminary conclusions on the efficiency of the proposed metamaterials and to identify the needs for further research.

2. Auxetic materials

Most of materials, which exist in nature, tend to get thinner to the direction of loading or excitation when stretched. In other words, as for elastic loadings, shrinkage usually appears in the direction which is perpendicular to the applied load. This behavior results in the reduction of the cross-sectional area of the structure. In case of compressive loadings, the exactly opposite effect appears. In this case, the cross-sectional area increases. The change of the length of the elastic material in the perpendicular direction with respect to the applied load, is given by the Poisson's ratio, which is usually a positive number taking values in the interval $(0, 0.5)$. This ratio is defined as the negative fraction of transverse strain $\Delta y/ly$ over the axial strain $\Delta x/lx$ [15]. However, there are materials which present exactly the opposite behavior. These materials, featuring a negative Poisson's ratio, are called auxetic materials and can be conceived as microstructures, which become thicker in the perpendicular direction to the one of the applied tensile loading. This is because of artificial joints inside the microstructure which in turn help flexing to occur [3, 14]. The attribute providing the auxetic behavior to these materials,

which occurs due to their specific internal structure, is the negative Poisson's ratio. This property is usually explained from the microstructure (star-shaped frames or inclusions), although other models have been used as well (chiral, perforated or mechanism-based).

The design of auxetic materials in the laboratory can be based on optimal design for the definition or fine-tuning of the auxetic microstructure. The effectiveness of these materials, as well as their response and adaptiveness to nonlinearities, can be verified by applying numerical homogenization tools and CAD/CAE software. A body, which presents an auxetic behavior, can consist of recurring patterns of identical microstructures as is usually the case in homogenization. Each microstructure consists of a monolithic body with specific geometry and a predefined deformation which integrates all the features of a compliant mechanism. In Fig. 1, the behavior of a conventional and an auxetic material, based on their microstructure, is shown.

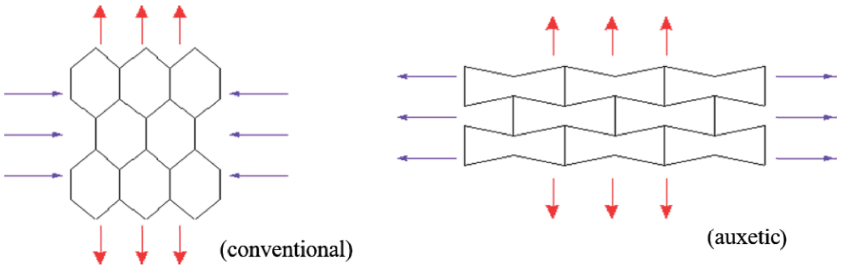

FIGURE 1. Conventional and auxetic materials.

The modern approach to design auxetics is based on topology optimization methods. For example, a topology optimized architecture with programmable Poisson's ratio over large deformations is presented and discussed in [2]. From the mathematical point of view, the optimization goal is defined as minimizing the error between the actual and the pre-defined value of Poisson's ratio over a range of discrete, nominal strain values. The topology optimized structures are designed and printed with programmable Poisson's ratios ranging from -0.8 to 0.8 over large deformations of $20\,\%$ or more. In addition, it is shown that with the combination of topology optimization with additive manufacturing, the design of new materials with desired properties is possible. A suitable topology optimization procedure for the optimum design of compliant mechanisms, using evolutionary-hybrid algorithms, and application to the design of auxetic materials has been proposed in Kaminakis et al. [9,10].

3. Applications of auxetic structures subjected to dynamic loads in comparison to conventional structures

3.1. Frequency analysis of conventional and auxetic structures. In the first investigation, damping plates made of conventional and auxetic microstructure are compared. For the finite element analysis, 4-node quadrilateral shell elements with reduced integration and large-strain formulation, are used for the discretization

of the core and the frontal sheets of the cell. Each node has six degrees of freedom. A lattice with conventional honeycomb-shaped core and a lattice with auxetic core are shown in Fig. 2. The main material of the cellular panel of the sandwich structure was chosen to be the A5052-H34 aluminum alloy due to its high stiffness. The material properties of this aluminum alloy are given in Table 1.

TABLE 1. Aluminum 5052–H34 properties

Material Properties	Young's Modulus (MPa)	Poisson's Ratio	Yield Strength (MPa)	Tensile Strength (MPa)	Shear Modulus (MPa)	Density (kg/mm^3)
	70330	0.36	213.7	262	25924.2	$2.68x10^{-6}$

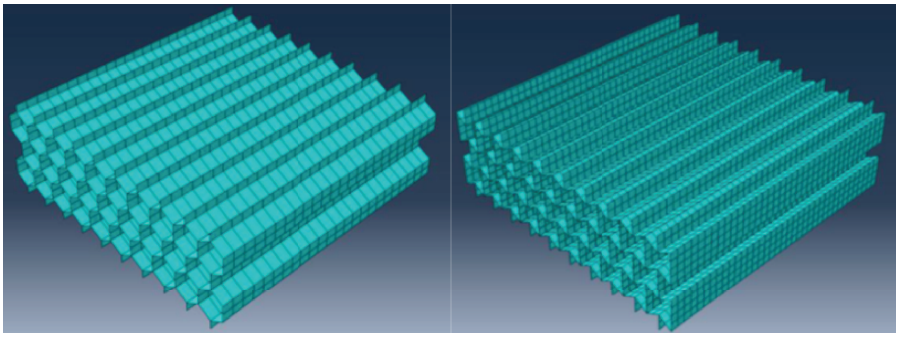

FIGURE 2. Discretized conventional (honeycomb) core and discretized auxetic core.

According to Gibson and Ashby [4], who proposed the properties of the cell based on the beam theory, a unitary cell of a cellular structure can be used for the prediction of the behaviour of the sandwich panel. The parameters of the unit cell are the height of the cell (h), the length of the cell wall (l), the depth of the cell wall (d) and the angle between the horizontal and the leaning cell wall. Moreover, the height ratio, and the depth ratio can be also calculated. For the conventional cell the angle is given as $\theta = 30$ degrees and the ratio $\alpha = 1$, while for the auxetic one the angle is given as $\theta = -30$ and $\alpha = 2$. The selection of the parameters of the auxetic cell has not been made arbitrarily, but in a manner that the behaviour of the auxetic simulates the function of a conventional cell, as the active coefficient is the same at the two vertical directions. These parameters for the conventional and the auxetic cell are given in Table 2.

The total dimensions of the conventional unit cell are given by:

$$L_c = \frac{2}{\cos\theta}$$
$$H_c = 2(h + l\sin\theta)$$

TABLE 2. Geometrical parameters of the conventional and the auxetic structure

Geometrical parameters	Conventional cell	Auxetic cell
Height of the cell wall, h (mm)	4.23	8.46
Leaning cell wall length, l (mm)	4.23	4.23
Depth of the cell wall, d (mm)	0.423	0.423
Cell angle, θ	30	30
Cell height ratio, α	1	2
Cell depth ratio, β	0.1	0.05

where L_c is the total length and H_c is the total height of the conventional unit cell.

Similarly, the total dimensions of the auxetic unit cell are given by:

$$L_a = 2l\cos\theta$$

$$H_a = 2(h - l\sin\theta)$$

where L_a is the total length and H_a is the total height of the auxetic unit cell.

Displacement-frequency results have been obtained through the frequency analysis. According to these results, the displacement of the node at the upper edge for the conventional and the auxetic structure have been recorded, respectively. It is noticed that the first eigenfrequencies, that is the ones where the maximum displacements occur, emerge in the interval of $0 - 5\,\text{Hz}$ for the conventional structure. Similarly, the first eigenfrequencies for the auxetic structure appear at the range $5 - 15\,\text{Hz}$. Moreover, in this case the peaks are scattered in this interval, in contrast to the previous case where the eigenfrequencies were concentrated. It is worth mentioning that the structure presents similar behavior at other nodes.

3.2. Design and Finite Element Analysis - Bullet Penetration test. Ashby and Gibson proposed the properties of the cell based on the beam theory and also discovered that a unitary cell of a cellular structure can be used as a prediction tool for the behavior of the sandwich panel [4]. Fig. 3 shows the unitary cell of both the conventional and the auxetic structure, along with the parameters that define the geometry of the cell. The main design parameters of the cell size are the height of the cell, the length of the cell wall, the thickness of the cell wall and the angle between the cell wall and the horizontal axis.

The first structure is characterized by a honeycomb structure without presenting any auxetic behavior. The structure consists of a set of cells in a 2×6 layout with dimensions $43.95 \times 20.27 \times 30\,\text{mm}$. The shape of the auxetic structure is characterized by the star shape, which has been chosen for the negative Poisson's ratio and consequently, its auxetic behavior. This particular structure was chosen because of its relatively simple shape that helps in its production with the utilization of additive manufacturing. The whole structure consists of a set of cells in a 2×7 arrangement with dimensions $43.53 \times 11.93 \times 30\,\text{mm}$. In both models, the sandwich panel is created by adding a front and a back panel of $0.5\,\text{mm}$ thickness.

In each Finite Element Analysis (FEA) model a 9 mm bullet at speed of 830 m/sec is used. The total duration of each study is 1 ms. The proper displacement restraint has been determined on the lateral surfaces of the two structures (symmetrically). The used material of the cellular structure is the A5052-H34 aluminum alloy due to its high stiffness. Table 1 shows the properties of the material.

The duration of each impact analysis is 1 ms and the bullet speed is 830 m/s, the deformation of the auxetic core is presented below (Fig. 4). The number of FE nodes is 40.991 and there are 20.614 elements of the model, while the number of time steps of the simulation is 25. Also, the type of finite elements is tetrahedral. FEA was performed using the Autodesk explicit analysis algorithm. The parametric model has been generated with the use of Autodesk Fusion 360 platform.

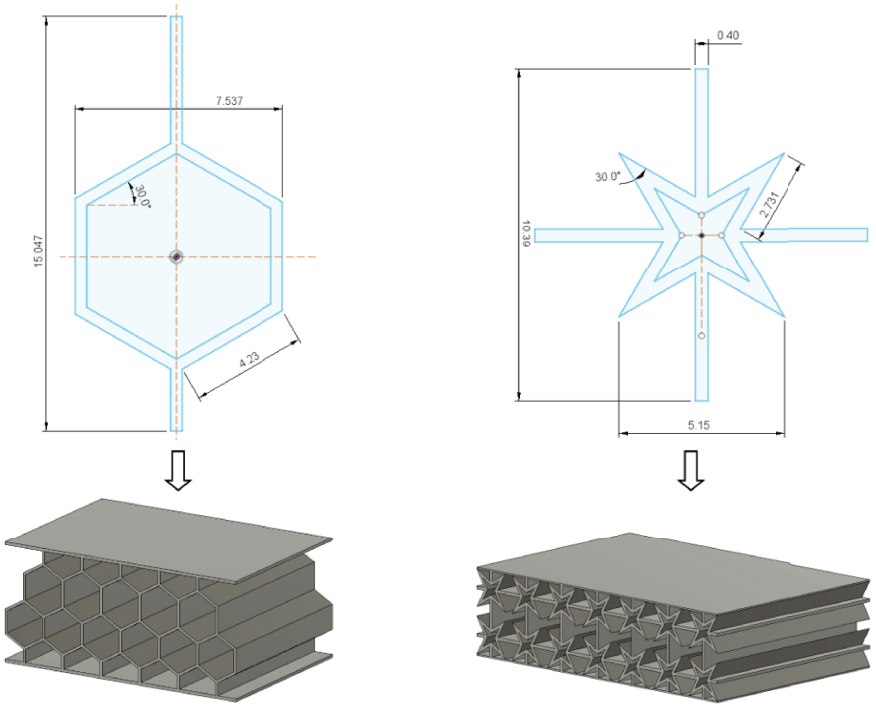

FIGURE 3. Non auxetic honeycomb structure and star-shaped auxetic structure.

In order to specify the effect of impact force on each structure we are going to present the maximum stress (Von Misses) and maximum displacement. Figure 5 shows the maximum stress on auxetic and conventional structure respectively. Figure 6 shows the maximum displacement on auxetic and conventional structure respectively.

For each structure, the stress on the top surface is higher than the bottom surface during the impact load period. After releasing the impact load, the stresses

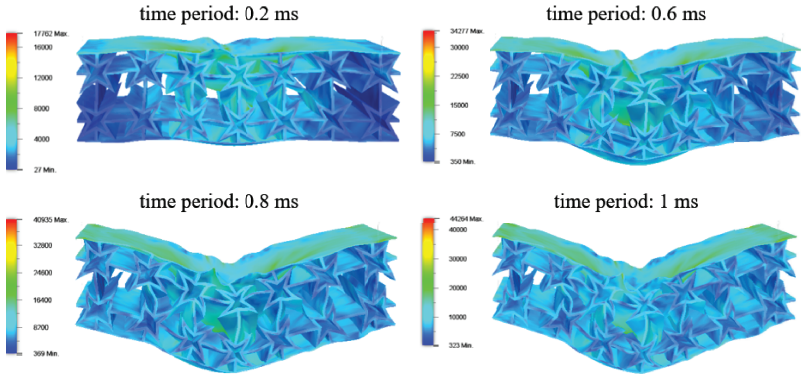

FIGURE 4. Bullet impact on the baseline auxetic star-shape sandwich panel.

on the bottom surfaces became lower for both the honeycomb and the star-shaped auxetic structure. From the results, we observe that during the study the material remains in the elastic region.

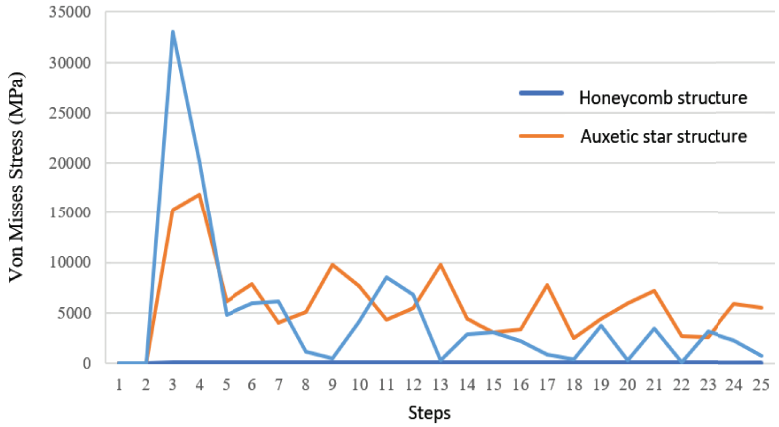

FIGURE 5. The impact von Misses stress of the upper surface of conventional honeycomb structure and auxetic star shape structure. The maximum stress on conventional structure is double compared with star shape structure.

3.3. Dynamic analysis of a wind turbine blade with auxetic components. The objective of this application is to investigate an important factor in the efficiency and operation of wind turbines, which is the operation of the blade and/or the rotor. Namely, the behavior of the materials that are used for absorbing/damping of the oscillation is studied.

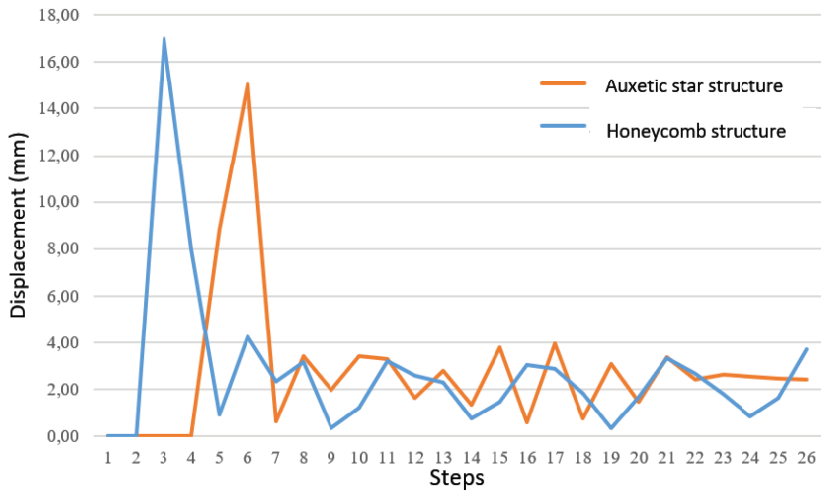

FIGURE 6. Displacement of the upper surface of conventional honeycomb structure and auxetic star shape structure.

TABLE 3. Materials properties for the blade model

Material Properties	Young's Modulus (MPa)	Poisson's Ratio	Density (kg/m^3)
Glass Fiber Plastic	70×10^3	0.259	2.8×10^3
Polymer Foam	27×10^3	0.34	270
Aluminum Foam	83×10^3	0.05	324
Auxetic material with star shaped microstructure	100×10^3	-0.35	270
E-GRP	2.3	0.25	2720

For this purpose, a 3-D model of the turbine blade is created, and harmonic loads are applied. Three cases of different materials, which are used for vibration damping, are compared. More specifically, a polymeric foam (modern high-performance material used for aerospace applications), an aluminum foam and an auxetic material (material with a negative Poisson's ratio) are considered. The properties of the three materials are given in Table 3.

The interior of the airfoil could be solid and its thickness could be calculated from the bending moment. At the fixed end the wind turbine, which is clamped to the hub, is subjected to compression and at the edge is subjected to tension. The material inside the blade is not subjected to compression and to tension, so it is considered hollow. The blade could ideally consist of two up-stream and down-stream to the wind direction lamina. However, this structure would not be functional for two reasons. Firstly, a continuous aerodynamic shape is necessary to achieve aerodynamic efficiency. Secondly, if the blade consists of two panels which are not fixed to each other, sliding phenomena could possibly occur leading

the structure to behave like two separate very thin blades. Thus, the two laminae should be fixed using beams or frames.

In the structural system of the blade, a composite frame with composite shear webs and spar caps from composite fiber reinforced plastic (E-GRP) has been chosen. The structure of the frame is shown in the section of the blade (see Fig. 7).

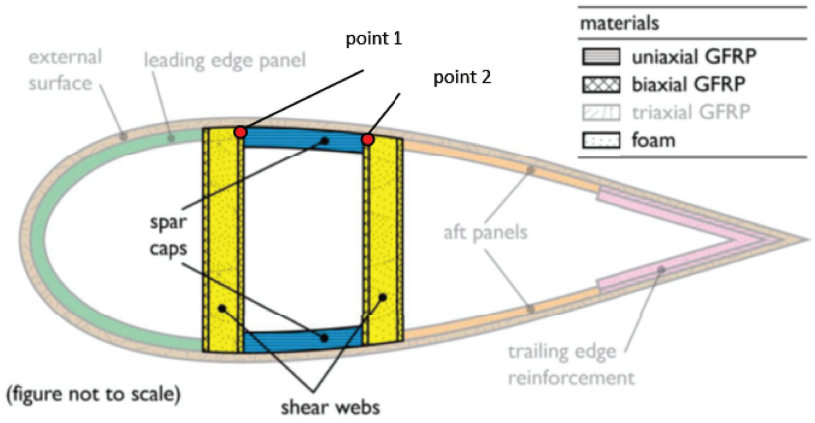

FIGURE 7. Section of the blade.

As shown in Fig. 7 the vertical beams are of sandwich type. This means that the material is a composite with two outer layers of fiber reinforced material (face material). The core material is a foam which is used due to its capability of achieving better absorption of harmonic loads and higher damping of the amplitudes. In this study, three different materials are considered in order to achieve the desired features: a polymer foam, an aluminum foam and an auxetic material.

The design of the supporting system is based on the geometry of the shell. The structural frame of the blade consists of two different materials; the E-GRP material for the spar caps, and the FRP material, which is used as an exterior material in composite vertical beams (shear webs). Also, composite beams are used as dampers. Three different cases are studied for the composite beams. The first case considers the use of a polymer foam for the beams, the second case an aluminum foam, and finally the third case considers the use of an auxetic material for the supporting beams. The results of the simulation are shown in comparative amplitude and phase diagrams. The first graph concerns the fluctuation of the amplitude of the three materials in relation to the frequency at two different points (see Fig. 7).

From Figs. 8 and 9 it appears that the three materials present a maximum point near the frequency of 6 Hz (6.5 Hz for the auxetic and the aluminum foam). At this frequency, the maximum energy absorption is due to resonance. Overall, one can conclude that the auxetic material presents lower amplitudes in contrast to the other two materials besides the resonance at 6.5 Hz. Moreover, the frequency is higher than the one of the aluminum foam, possibly due to the increased strength

in stress which in turn is due to the negative Poisson's ratio. Lastly, after the resonance point and until 8.5 Hz there is a discontinuity between point 1 and 2. The reason of this discontinuity lies in to the aerodynamic profile of the blade.

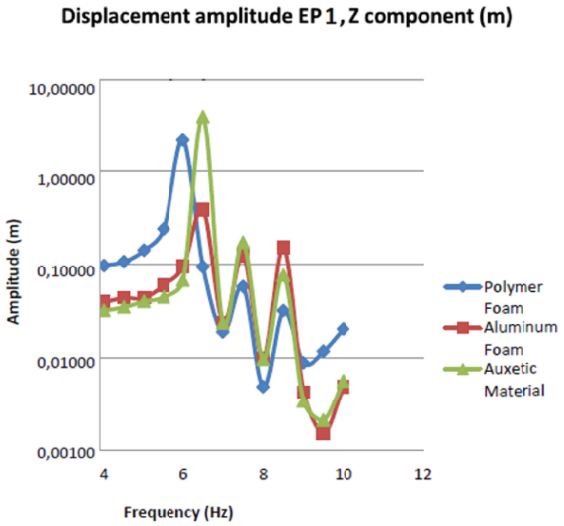

FIGURE 8. Amplitude-frequency graph for the three materials at point 1.

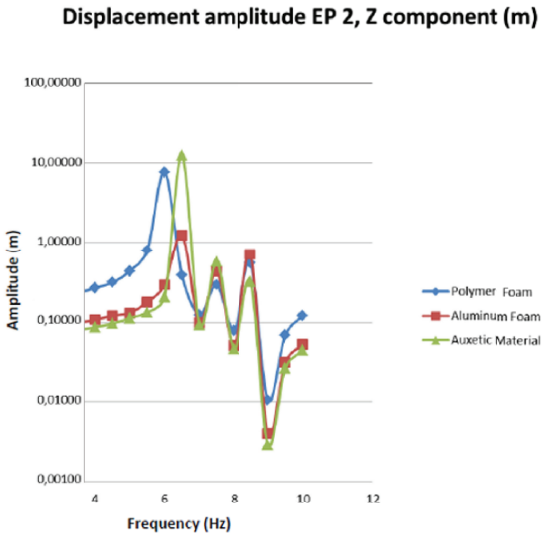

FIGURE 9. Amplitude-frequency graph for the three materials at point 2.

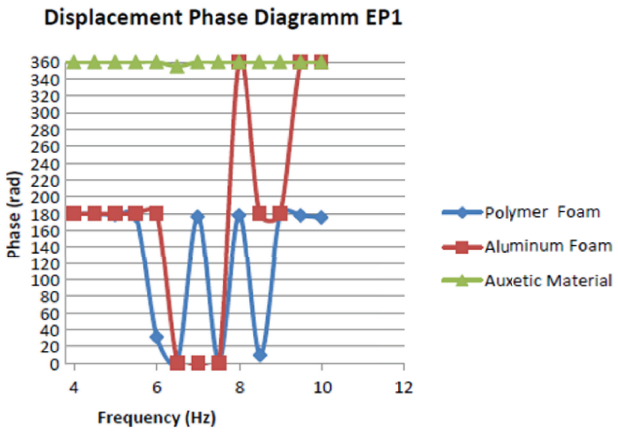

FIGURE 10. Phase difference diagram for the three materials at point 1.

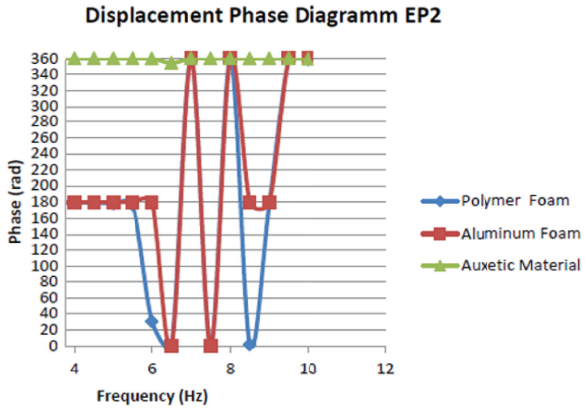

FIGURE 11. Phase difference diagram for the three materials at point 2.

The diagrams in Figs. 10 and 11 present the comparison in the phase difference of the three materials in different load frequencies for two different points of the structure respectively (see Fig. 7).

In both cases the auxetic material has almost a constant phase at 360°. This coincides with the 0° because of the trigonometric circle and the explanation lies in the negative Poisson's ratio and its behavior at the deformations. For the other two materials we observe that up to the maximum load the phase is approximately (180°) until the resonance. Generally, from the phase difference graph in comparison with the amplitude diagrams one can observe that the auxetic material presents a very efficient response as a vibration damper, with the aluminum foam

coming next. It should be noted that the auxetic material shows higher Von Misses stress values than the other materials; however it avoids the critical limits of the structure.

4. Conclusions

From the numerical experiments of the present investigation, it was shown that auxetic materials present unique mechanical behavior, which is based on negative Poisson's ratio of the cell structures. The frequency analysis of auxetic materials, and more specifically the results of the simulations carried out through commercial finite element software, suggested that the auxetic panel presents higher resistance to strain in comparison to the one with the conventional core. Based on the results of the dynamic analysis one can observe that for the same excitation the conventional model presents bigger displacements in contrast to the auxetic model. Moreover, in the case of the conventional model, the resonance phenomenon takes place in a lower range of frequencies. This conclusion came up from the observation that the peaks for this model appear for much lower frequencies compared to the auxetic model. All the above indicate that the structures with the auxetic core have an advantage over the conventional, which is ones due to the special characteristics of the auxetic core structure.

In the second application the effectiveness of the star-shaped structure on bullet penetration test was investigated. The results showed that even if the structure was subjected to extremely high impact loads, the auxetic materials presented very good behavior. According to the results, on the front surface of the auxetic structure the movement is smaller and on the back surface the movement value is lower in relation to the maximum values. Thus, it is noted, that the rate of the vibration damping is smoother in the auxetic structure, compared to the non-auxetic, where a constant movement is present during the analysis. It was also shown that a significantly higher Von Mises stresses are measured at the non-auxetic structure.

From the dynamic analysis of the auxetic wind turbine blade, and according to the comparative graphs, it was found that the best damping behaviour is achieved by the auxetic material. The microstructure, due to its auxetic properties, was proved to be very efficient to the absorption of the oscillations providing immediate response to the excitations with the minimum total amplitude. The resonance point, at the frequency of 6.5 Hz, gives the ability of absorbing energy without any impact on the integrity of the structure according to the deformation.

Future investigation will consider the usage of other auxetic microstructures and materials in order to meet specific tasks, as well as the influence of plasticity and other nonlinear effects. Moreover, the properties of auxetic materials coming from topology optimization and their applicability for damping applications can be further investigated as well. In fact, in this preliminary investigation the choice of the microstructure is based on experience and trial-and-error investigation. A more detailed approach could be based on a band gap analysis for the required frequency content [11] in combination with parametric analysis and optimal design. For parametric optimal design for the case of optimal damping, the loss factor could serve as the frequency function, in order to carry out an analysis in a wider range

of frequencies. Similarly, in penetration studies the total absorbed energy and plastification can be used as optimization task.

Acknowledgments. The research of the first author is co-financed by Greece and the European Union (European Social Fund- ESF) through the Operational Programme "Human Resources Development, Education and Lifelong Learning" in the context of the project "Reinforcement of Postdoctoral Researchers - 2nd Cycle" (MIS-5033021), implemented by the State Scholarships Foundation IKY.

References

1. A. Alomarah, S. Xu, S. Masood, D. Ruan, *Dynamic performance of auxetic structures: experiments and simulation*, Smart Materials and Structures **29** (2020), 055031.
2. A. Clausen, F. Wang, J. S. Jensen, O. Sigmund, J. A. Lewis, *Topology Optimized Architectures with Programmable Poisson's Ratio over Large Deformations*, Advanced Materials **27** (2015), 5523–5527.
3. K. E. Evans, *Design of doubly-curved sandwich panels with honeycomb cores*, Composite Structures **17** (1991), 95–111.
4. L. J. Gibson, M. F. Ashby, *Cellular solids: Structure and Properties*, Cambridge University Press, Cambridge, 1988.
5. S. C. Han, D. S. Kang, T. K. Kang, *Two nature-mimicking auxetic materials with potential for high energy absorption*, Materials Today **26** (2019), 30–39.
6. G. Imbalzano, J. P. Tran, T. N. Ngo, P. V. S. Lee, *A numerical study of auxetic composite panels under blast loadings*, Composite Structures **135** (2016), 339–352.
7. G. Imbalzano, J. P. Tran, T. N. Ngo, P. V. S. Lee, *Three-dimensional modelling of auxetic sandwich panels for localised impact resistance*, Journal of Sandwich Structures & Materials **19** (2017), 291–316.
8. G. Imbalzano, S. Linforth, T. N. Ngo, P. V. S. Lee, J. P. Tran, *Blast resistance of auxetic and honeycomb sandwich panels: Comparisons and parametric designs*, Composite Structures **183** (2018), 242–261.
9. N. T. Kaminakis, G. E. Stavroulakis, *Topology optimization for compliant mechanisms, using evolutionary-hybrid algorithms and application to the design of auxetic materials*, Composites Part B **43** (2012), 2655–2668.
10. N. T. Kaminakis, G. A. Drosopoulos, G. E. Stavroulakis, *Design and verification of auxetic microstructures using topology optimization and homogenization*, Arch. Appl. Mech. **85** (2015), 1289–1306.
11. P. Koutsianitis, G. K. Tairidis, G. A. Drosopoulos, G. E. Stavroulakis, *Conventional and star-shaped auxetic materials for the creation of band gaps*, Arch. Appl. Mech. **89** (2019), 2545–2562.
12. P. R. Madke, R. Chowdhury, *Anti-impact behavior of auxetic sandwich structure with braided face sheets and 3D re-entrant cores*, Composite Structures **236** (2020), 111838.
13. G. E. Stavroulakis, *Auxetic behaviour: appearance and engineering applications*, Physica status solidi (b) **242** (2015), 710—720.
14. P. S. Theocaris, G. E. Stavroulakis, P. D. Panagiotopoulos, *Negative Poisson's ratios in composites with star-shaped inclusions: a numerical homogenization approach*, Arch. Appl. Mech. **67** (1997), 274–286.
15. H. Wan, H. Ohtaki, S. Kotosaka, G. M. Hu, *A study of negative Poisson's ratios in auxetic honeycombs based on a large deflection model*, Eur. J. Mech., A, Solids **23** (2004), 95–106.
16. W. Wu, W. Hu, G. Qian, H. Liao, X. Xu, F. Berto, *Mechanical design and multifunctional applications of chiral mechanical metamaterials: A review*, Materials & Design **180** (2019), 107950.
17. C. Yang, H. D. Vora, Y. Chang, *Behavior of auxetic structures under compression and inpact forces*, Smart Materials and Structures **27** (2018), 025012.

АУКСЕТИЧНИ МЕТАМАТЕРИЈАЛИ ПОД ДИНАМИЧКИМ ОПТЕРЕЋЕЊЕМ

Резиме. Материјали са негативним Пуасоновим односом називају се ауксетични и имају побољшана својства (нпр. пригушивање, отпорност на удубљење, жилавост на лом и отпорност на удар) под спољним оптерећењима. Ауксетична својства су изведена из микроструктура необичног облика, као што су рамови у облику звезде. У овом раду су развијени модели коначних елемената за динамичку анализу ауксетичних микроструктура. Прво је представљен модел који се односи на ауксетичне микроструктуре, за језгро структуралних панела. Затим се разматра употреба ауксетичних материјала у оклопним плочама у проблемима са динамичким продором метка. На крају, извршена је нумеричка симулација лопатица ветротурбина, са алуминијумском пеном, полимерном пеном и предложеним ауксетичним материјалом. Нумерички резултати показују да употреба ауксетичних микроструктура резултира побољшаним динамичким одзивом система у поређењу са конвенционалним материјалима.

(Received 03.11.2021.)
(Revised 21.01.2022.)
(Available online 06.04.2022.)

School of Production Engineering and Management
Technical University of Crete
Chania
Greece

Department of Mechanical Engineering
Hellenic Mediterranean University
Heraklion
Greece

Technical University of Crete
Greece
ntintakis@isc.tuc.gr

Discipline of Civil Engineering
University of Central Lancashire
Preston
North West England

Discipline of Civil Engineering
University of KwaZulu-Natal
Durban
South Africa
gdrosopoulos@uclan.ac.uk, drosopoulosg@ukzn.ac.za

School of Production Engineering and Management
Technical University of Crete
Chania
Greece
panoskout@gmail.com

School of Production Engineering and Management
Technical University of Crete
Chania
Greece
gestavr@dpem.tuc.gr